HHS Public Access

Author manuscript

*J Urol*. Author manuscript; available in PMC 2018 February 07.

Published in final edited form as:

*J Urol*. 2018 January ; 199(1): 126–132. doi:10.1016/j.juro.2017.07.070.

# Prostate Specific Membrane Antigen Targeted $^{18}$F-DCFPyL Positron Emission Tomography/Computerized Tomography for the Preoperative Staging of High Risk Prostate Cancer: Results of a Prospective, Phase II, Single Center Study

**Michael A. Gorin**[*,†], **Steven P. Rowe**[†], **Hiten D. Patel**, **Igor Vidal**, **Margarita Mana-ay**, **Mehrbod S. Javadi**, **Lilja B. Solnes**, **Ashley E. Ross**, **Edward M. Schaeffer**, **Trinity J. Bivalacqua**, **Alan W. Partin**, **Kenneth J. Pienta**[†], **Zsolt Szabo**, **Angelo M. De Marzo**, **Martin G. Pomper**[†], and **Mohamad E. Allaf**

James Buchanan Brady Urological Institute (MAG, HDP, MM-a, AER, TJB, AWP, KJP, MEA), Departments of Urology (MAG, HDP, MM-a, AER, TJB, AWP, KJP, MEA) and Pathology (IV, AMDM) and The Russell H. Morgan Department of Radiology and Radiological Science (SPR, MSJ, LBS, ZS, MGP), The Johns Hopkins University School of Medicine, Baltimore, Maryland, and Department of Urology, Northwestern University Feinberg School of Medicine (EMS), Chicago, Illinois

## Abstract

**Purpose—**We prospectively evaluated the diagnostic performance of prostate specific membrane antigen targeted $^{18}$F-DCFPyL positron emission tomography/computerized tomography in the preoperative staging of men at high risk for harboring metastatic prostate cancer despite a negative conventional staging evaluation.

**Materials and Methods—**Men with clinically localized high or very high risk prostate cancer were imaged with $^{18}$F-DCFPyL positron emission tomography/computerized tomography before undergoing radical prostatectomy with standardized pelvic lymph node dissection. The scans were interpreted by 2 blinded nuclear medicine readers and assessed for interreader variability as well as diagnostic accuracy for pelvic lymph node staging. Surgical pathology served as the reference standard to which $^{18}$F-DCFPyL scan findings were compared.

**Results—**A total of 25 men contributed analyzable data to this study. Seven of these patients (28%) were found to have 1 or more positive lymph nodes on surgical pathology. Sites of radiotracer uptake were identified in the prostate of all imaged patients. The 2 readers identified the same number of prostatic lesions in 22 patients (88%), of whom all had at least 1 intraprostatic lesion in common between the 2 reads. Additionally, the readers assigned the same N stage to 46

[*]Correspondence: 600 North Wolfe St., Park 213, Baltimore, Maryland 21287 (telephone: 410-502-7710; FAX: 410-502-7711; mgorin1@jhmi.edu).

[†]Financial interest and/or other relationship with Progenics Pharmaceuticals.

No direct or indirect commercial incentive associated with publishing this article.

The corresponding author certifies that, when applicable, a statement(s) has been included in the manuscript documenting institutional review board, ethics committee or ethical review board study approval; principles of Helsinki Declaration were followed in lieu of formal ethics committee approval; institutional animal care and use committee approval; all human subjects provided written informed consent with guarantees of confidentiality; IRB approved protocol number; animal approved project number.

of 50 individual lymph node packets (92%). Following reconciliation of the relatively few discordant imaging reads, 7 patients (28%) were found to have 1 or more sites of radiotracer uptake in the pelvis consistent with N1 disease, resulting in 71.4% sensitivity (95% CI 29.0–96.3) and 88.9% specificity (95% CI 65.3–98.6). Analysis at the level of individual nodal packets resulted in 66.7% sensitivity (95% CI 29.9–92.5) and 92.7% specificity (95% CI 80.1–98.5). Three men (12%) had evidence of M1a disease.

**Conclusions—**$^{18}$F-DCFPyL positron emission tomography/computerized tomography allowed for accurate detection of prostate cancer sites in men believed to have clinically localized disease based on conventional imaging. Our results support the need for a larger study to more precisely define the diagnostic accuracy of this novel molecular imaging test.

## Keywords

prostatic neoplasms; 2-(3-(1-carboxy-5-((6-fluoropyridine-3-carbonyl)amino)pentyl)ureido) pentanedioic acid; positron-emission tomography; tomography; X-ray computed; diagnosis

Definitive local treatment with radical prostatectomy or radiation therapy remains the standard of care in men with intermediate or high risk PCa.[1–3] Prior to undergoing treatment patients at risk for harboring metastatic PCa should undergo a staging evaluation using a combination of $^{99m}$Tc-methylene diphosphonate bone scan as well as pelvic imaging with CT or MRI. Current guidelines recommend a risk adapted approach to the use of staging imaging in men newly diagnosed with PCa, taking into account pretreatment serum PSA level, clinical T stage and biopsy Gleason sum.[1–3]

However, despite appropriate staging imaging use up to 30% of men with high risk PCa will be found to have clinically occult lymph node metastases at radical prostatectomy.[4,5] Additionally, a significant proportion of men will have persistently elevated PSA or biochemical recurrence following surgery.[6–9] In the absence of positive surgical margins these treatment failures can be attributed to sites of extraprostatic disease that escaped detection by conventional imaging at the time of initial cancer staging.

In an effort to improve the accuracy of currently available modalities of PCa imaging there has been growing interest in PET.[10] A number of novel PET radiotracers have been explored for this purpose.[11,12] Most promising among them is the class of radiotracers targeting PSMA, a type II glycoprotein that is over expressed in more than 95% of prostate tumors.[13,14] To date, the majority of work on PSMA targeted PET imaging has been performed using the urea based small molecule $^{68}$Ga-PSMA-11, also known as $^{68}$Ga-PSMA-HBED-CC. However, there are several limitations related to using $^{68}$Ga as a PET radionuclide, including the inability to produce large batch quantities of radiotracer and distribution of the agent to distant imaging centers.

These issues can be addressed using alternative $^{18}$F labeled radiotracers.[15,16] Indeed, multiple fluorinated compounds targeting PSMA have been developed.[17,18] Furthest along in clinical development is the $^{18}$F-DCFPyL radiotracer, which was first described by Chen et al.[19] This radiotracer has been examined in several studies in the context of imaging biochemically recurrent or metastatic PCa.[20–22]

We report the results of a prospective, phase II, single center study evaluating the diagnostic performance of $^{18}$F-DCFPyL PET/CT in the preoperative staging of men at high risk for harboring metastatic PCa despite a negative staging evaluation with conventional imaging.

## PATIENTS AND METHODS

This study was approved by The Johns Hopkins Medical Institutions institutional review board (NA_00092956/J1418) as an extension of a previously completed, first in human study evaluating the $^{18}$F-DCFPyL radiotracer (ClinicalTrials.gov Identifier NCT02151760).[20] All study procedures were done in accordance with the Declaration of Helsinki and the International Conference on Harmonisation of Good Clinical Practice.

Men with clinically localized high or very high risk PCa as defined by the NCCN®[3] were eligible for this study. Pre-enrollment clinical stage was determined with $^{99m}$Tc-methlyene diphosphonate bone scan as well as CT or MRI of the pelvis. In accordance with recommendations from the PCWG3 (Prostate Cancer Clinical Trials Working Group 3)[23] lymph nodes measuring greater than 15 mm in axial diameter were considered pathologically enlarged. Patients with such findings on cross-sectional imaging were deemed ineligible for this study.

Upon signing informed consent, patients underwent $^{18}$F-DCFPyL PET/CT as previously described.[20] In brief, 1 hour after intravenous administration of approximately 9 mCi $^{18}$F-DCFPyL radiotracer, a PET/CT scan was acquired from the mid thigh to the vertex of the skull. Of note, patients were asked to void prior to imaging to decrease bladder activity. Radiotracer for this study was synthesized locally at our center using the method previously described by Ravert et al.[24]

One to 7 days after PET/CT radical prostatectomy with bilateral pelvic lymph node dissection was performed by 1 of 5 expert urological oncologists. The overall surgical technique (ie robotic vs open) was determined at the discretion of the treating surgeon. Regardless of surgical approach, all lymph node dissections were performed using a standardized anatomical template (supplementary figure, http://jurology.com/), which resulted in removal of 2 lymph node packets per patient (ie 1 per side of the pelvis). At the completion of the study 2 genitourinary pathologists (AMDM and IV) blinded to imaging results collaboratively reviewed the surgical specimens.

Two blinded nuclear medicine readers (MSJ and LBS) independently read the $^{18}$F-DCFPyL PET/CT scans in separate random orders. These reads were assessed for concordance of the number of lesions located in the prostate gland, overall N stage, N stage on each side of the pelvis and M stage. All cases with discordant N or M stage between the 2 reads were then reconciled by collaborative rereview.

Using surgical pathology as the reference standard the parameters calculated with respect to lymph node staging were sensitivity, specificity, and positive and negative predictive values. This analysis was performed at the level of the 25 patients overall as well as the 50 individual lymph node packets. Calculations were performed with MedCalc®, version 17.1.

## RESULTS

A total of 28 patients were enrolled in this study between March 2015 and September 2016, and no adverse events were encountered during the study. Complete analyzable data were available on 25 enrolled patients (89.3%). One patient was excluded from analysis after he was mistakenly enrolled with metastatic disease found on conventional imaging. Another patient was excluded from study after we learned that staging imaging had been done 8 months preoperatively, leaving clinical stage at prostatectomy open to question. Finally, a third patient was excluded because pelvic lymph node dissection could not be safely performed due to a large iliac artery aneurysm.

Table 1 shows detailed characteristics of the 25 patients included in analysis. Median patient age was 61 years (range 49 to 75) and median PSA was 9.3 ng/ml (range 3.6 to 125.5) at the time of study enrollment. On biopsy before prostatectomy Gleason score was 4 + 5 = 9 or 5 + 4 = 9 in 13 study subjects (52%). Additionally, 14 men (56%) had palpable disease on digital rectal examination (ie cT2a or greater) and 8 (32%) met the definition of having very high risk PCa.

Following radical prostatectomy 18 patients (72%) were found to have Gleason 4 + 5 = 9 or 5 + 4 = 9 PCa (table 1). In terms of primary tumor staging 13 cases (52%) were pT3a and 7 (28%) were pT3b. A median of 13 lymph nodes (range 5 to 45) were removed at surgery. Seven men (28%) were found to have 1 or more positive lymph nodes. Notably, 2 of these patients (29%) had bilateral lymph node involvement, resulting in a total of 9 positive lymph packets. A median of 3 disease involved lymph nodes (range 1 to 7) were found in each positive nodal packet. Positive lymph nodes were typically small with a median diameter of 3 mm (range 1 to 12).

With respect to $^{18}$F-DCFPyL PET/CT findings 1 reader detected 32 discrete intraprostatic lesions among the 25 imaged patients. These lesions had a median $SUV_{max}$ of 7.0 (range 3.0 to 40.2). The second reader detected 29 intraprostatic lesions with a median $SUV_{max}$ of 6.6 (range 3.3 to 37.8). The 2 readers identified the same number of lesions in 22 cases (88%) and all cases had at least 1 intraprostatic lesion in common between the 2 reads. Additionally, the readers assigned the same N stage to 46 of the 50 individual lymph node packets (92%) and to 22 of the 25 cases overall (88%). Finally, 24 patients (96%) were assigned the same clinical M stage. Figures 1 and 2 show representative images of patients believed to have localized and distant disease, respectively, based on $^{18}$F-DCFPyL PET/CT.

After reconciling the relatively few discordant reads, 7 patients (28%) were found to have 1 or more sites of focal radiotracer in the pelvis consistent uptake in the pelvis consistent with N1 disease, resulting in 71.4% sensitivity (95% CI 29.0–96.3) and 88.9% specificity (95% CI with N1 disease. This resulted in 71.4% sensitivity (95% CI 29.0–96.3) and 88.9% specificity (95% CI 65.3–98.6) for the imaging test (table 2). Similar results were found on analysis at the individual packet level with 66.7% sensitivity (95% CI 29.9–92.5) and 92.7% specificity (95% CI 80.1–98.5). Additionally, the readers determined that 3 patients (12%) had PET/CT findings consistent with M1a disease.

## DISCUSSION

In this study we prospectively evaluated the diagnostic performance of $^{18}$F-DCFPyL PET/CT to preoperatively stage high risk PCa in men believed to have clinically localized disease based on conventional imaging. This represents the first study to evaluate this novel imaging test in the setting of preoperative PCa staging.

$^{18}$F-DCFPyL PET/CT correctly identified 5 of 7 cases (71.4%) with otherwise clinically occult positive lymph nodes while over staging only 2 cases (8%). To place the observed sensitivity value in context, 50% of disease involved lymph nodes were less than 3 mm. Perhaps more importantly, $^{18}$F-DCFPyL PET/CT identified putative sites of distant metastases in 3 men (12%). Finally, this novel imaging test identified discrete foci of abnormal radiotracer uptake in the prostate gland of all imaged patients. Given the normal biodistribution and the low background uptake of the radiotracer, these sites likely corresponded to areas of PCa. This finding suggests that this imaging test can be used to aid in the topographic mapping of cancer in the prostate and in fact other PSMA targeted radiotracers have shown promise for this purpose.[10,13,14]

As with any new imaging test, it is important to understand its performance characteristics with respect to interreader variability. In this study we observed a high degree of concordance between our 2 readers in terms of detecting local and distant sites of disease. We believe that the readers were able to achieve this high level of concordance between reads due to the low blood pool and the background activity of the $^{18}$F-DCFPyL radiotracer. Given this, the lesions, even those with low SUV values, had a high degree of conspicuity, allowing for high confidence calls by the readers.

However, an area of particular difficulty for readers was the assessment of pelvic lymph nodes located near the ureters. Like many agents used for molecular imaging, $^{18}$F-FCFPyL is excreted in urine, making focal uptake difficult at times to discern from activity in the ureters. In our study 2 of the 3 false-positive radiotracer uptake sites (66.7%) were confirmed to be located in the ureters upon further review by a third highly experienced reader (SPR).

We suspect that with additional experience the specificity of this imaging test will improve as readers develop a framework for discerning ureteral activity. In fact, recent data on $^{68}$Ga-PSMA-11 PET/CT showed that increasing reader experience positively correlated with interreader agreement and presumably with accuracy to determine clinical stage.[25] The specificity of $^{18}$F-DCFPyL PET/CT may also be improved through concurrent use of pelvic MRI, multiple imaging time points and/or administration of diuretics.

We are not alone in our observations regarding the diagnostic potential of PSMA targeted PET in the preoperative setting. A review of the literature revealed 4 studies that evaluated $^{68}$Ga-PSMA-11 PET/CT for lymph node staging prior to radical prostatectomy.[26–29] Together these studies include data on 210 men, of whom 35.2% had pN1 disease. Meta-analysis of these studies demonstrated similar sensitivity between the $^{68}$Ga-PSMA-11 and $^{18}$F-DCFPyL radiotracers for preoperative lymph node staging (Supplementary Methods, and supplementary tables 1 and 2, http://jurology.com/). More specifically 61.6% sensitivity

(95% CI 44.2–77.8) was observed for $^{68}$Ga-PSMA-11 PET/CT to determine overall pN1 stage. However, the $^{68}$Ga-PSMA-11 radiotracer had a slightly higher observed specificity of 97.6% (95% CI 89.7–100). In an analysis of individual lymph node packets sensitivity and specificity were found to be 61.4% (95% CI 39.4–81.4) and 97.8% (95% CI 93.9–100), respectively. The results of this meta-analysis suggest that PET/CT with $^{18}$F-DCFPyL offers diagnostic performance similar to that of $^{68}$Ga-PSMA-11. This observation strengthens our confidence in the findings of our relatively small study both of these radiotracers are urea based small molecules that bind to the catalytic domain of the PSMA protein.[30]

Our study is not without limitations, foremost being the small sample size of only 25 patients. Another limitation is the lack of prostate whole mounts to confirm that radiotracer uptake in the prostate glands localized to sites of cancer. Along these lines, we lacked histological proof in the 3 cases reclassified with M1a disease.

Despite these limitations, a considerable strength of our study is its prospective design, which is in contrast to the existing literature on PSMA targeted imaging which mostly includes retrospective studies.[13,14] An additional strength is our use of surgical pathology as the reference standard in the analysis of diagnostic accuracy for lymph node staging.

## CONCLUSIONS

We provide the first prospective evaluation of PSMA targeted PET/CT using the $^{18}$F-DCFPyL radiotracer in the preoperative staging of men with clinically localized PCa. This novel imaging test identified sites of radiotracer uptake in the prostate gland of all imaged patients and allowed for the accurate detection of otherwise occult lymph node metastases. Moreover, a subset of men were identified with evidence of occult distant metastatic disease. A large confirmatory multicenter trial is currently under way to more definitively determine the diagnostic performance of this test for imaging local and distant sites of PCa (ClinicalTrials.gov identifier NCT02981368).

## Supplementary Material

Refer to Web version on PubMed Central for supplementary material.

## Acknowledgments

This study was supported by Progenics Pharmaceuticals, Inc., charitable donations to The James Buchanan Brady Urological Institute and National Cancer Institute CA134675.

W. Fendler, S. Leyh-Bannurah, L. Budaeus and T. Maurer provided clarifying data included in the meta-analysis.

## Abbreviations and Acronyms

| | |
|---|---|
| **CT** | X-ray computerized tomography |
| **MRI** | magnetic response imaging |
| **PCa** | prostate cancer |
| **PET** | positron emission tomography |

| | |
|---|---|
| **PSA** | prostate specific antigen |
| **PSMA** | prostate specific membrane antigen |
| **SUV** | standardized uptake value |
| **$SUV_{max}$** | maximum SUV |

## References


1. Thompson I, Thrasher JB, Aus G, et al. Guideline for the management of clinically localized prostate cancer: 2007 update. J Urol. 2007; 177:2106. [PubMed: 17509297]
2. Mottet N, Bellmunt J, Bolla M, et al. EAU-ESTRO-SIOG guidelines on prostate cancer. Part 1: screening, diagnosis, and local treatment with curative intent. Eur Urol. 2016; 71:1. [PubMed: 27471164]
3. [Accessed April 15, 2017] NCCN Clinical Practice Guidelines in Oncology, Prostate Cancer Version 2.2017. Available at https://www.nccn.org/professionals/physician_gls/pdf/prostate.pdf
4. Briganti A, Larcher A, Abdollah F, et al. Updated nomogram predicting lymph node invasion in patients with prostate cancer undergoing extended pelvic lymph node dissection: the essential importance of percentage of positive cores. Eur Urol. 2012; 61:480. [PubMed: 22078338]
5. Tosoian JJ, Chappidi M, Feng Z, et al. Prediction of pathological stage based on clinical stage, serum prostate-specific antigen, and biopsy Gleason score: Partin tables in the contemporary era. BJU Int. 2017; 119:676. [PubMed: 27367645]
6. Reese AC, Pierorazio PM, Han M, et al. Contemporary evaluation of the national comprehensive cancer network prostate cancer risk classification system. Urology. 2012; 80:1075. [PubMed: 22995570]
7. Sundi D, Wang V, Pierorazio PM, et al. Identification of men with the highest risk of early disease recurrence after radical prostatectomy. Prostate. 2014; 74:628. [PubMed: 24453066]
8. Joniau S, Briganti A, Gontero P, et al. Stratification of high-risk prostate cancer into prognostic categories: a European multi-institutional study. Eur Urol. 2015; 67:157. [PubMed: 24486307]
9. Pompe RS, Karakiewicz PI, Tian Z, et al. Oncologic and functional outcomes after radical prostatectomy for high or very high risk prostate cancer: European validation of the current NCCN® guideline. J Urol. 2017; 198:354. [PubMed: 28216329]
10. Gorin MA, Rowe SP, Denmeade SR. Clinical applications of molecular Imaging in the management of prostate cancer. PET Clin. 2017; 12:185. [PubMed: 28267452]
11. Mertan FV, Lindenberg L, Choyke PL, et al. PET imaging of recurrent and metastatic prostate cancer with novel tracers. Future Oncol. 2016; 12:2463. [PubMed: 27527923]
12. Lindenberg L, Choyke P, Dahut W. Prostate cancer imaging with novel PET tracers. Curr Urol Rep. 2016; 17:18. [PubMed: 26874530]
13. Maurer T, Eiber M, Schwaiger M, et al. Current use of PSMA-PET in prostate cancer management. Nat Rev Urol. 2016; 13:226. [PubMed: 26902337]
14. Rowe SP, Gorin MA, Allaf ME, et al. PET imaging of prostate-specific membrane antigen in prostate cancer: current state of the art and future challenges. Prostate Cancer Prostatic Dis. 2016; 19:223. [PubMed: 27136743]
15. Sanchez-Crespo A. Comparison of gallium-68 and fluorine-18 imaging characteristics in positron emission tomography. Appl Radiat Isot. 2013; 76:55. [PubMed: 23063597]
16. Gorin MA, Pomper MG, Rowe SP. PSMA-targeted imaging of prostate cancer: the best is yet to come. BJU Int. 2016; 117:715. [PubMed: 27079480]
17. Rowe SP, Drzezga A, Neumaier B, et al. Prostate-specific membrane antigen-targeted radiohalogenated PET and therapeutic agents for prostate cancer. J Nucl Med, suppl. 2016; 57:90S.
18. Rowe SP, Gorin MA, Fragomeni RAS, et al. Clinical experience with $^{18}$F-labeled small molecule Inhibitors of prostate-specific membrane antigen. PET Clin. 2017; 12:235. [PubMed: 28267456]

19. Chen Y, Pullambhatla M, Foss CA, et al. 2-(3-{1-Carboxy-5-[(6-[$^{18}$F]fluoro-pyridine-3-carbonyl)-amino]-pentyl}-ureido)-pentanedioic acid, [$^{18}$F] DCFPyL, a PSMA-based PET imaging agent for prostate cancer. Clin Cancer Res. 2011; 17:7645. [PubMed: 22042970]
20. Szabo Z, Mena E, Rowe SP, et al. Initial evaluation of [$^{18}$F]DCFPyL for prostate-specific membrane antigen (PSMA)-targeted PET imaging of prostate cancer. Mol Imaging Biol. 2015; 17:565. [PubMed: 25896814]
21. Dietlein M, Kobe C, Kuhnert G, et al. Comparison of [$^{18}$F]DCFPyL and [$^{68}$Ga]Ga-PSMA-HBED-CC for PSMA-PET imaging in patients with relapsed prostate cancer. Mol Imaging Biol. 2015; 17:575. [PubMed: 26013479]
22. Dietlein F, Kobe C, Neubauer S, et al. PSA-stratified performance of $^{18}$F- and $^{68}$Ga-labeled tracers in PSMA-PET imaging of patients with biochemical recurrence of prostate cancer. J Nucl Med. 2017; 58:947. [PubMed: 27908968]
23. Scher HI, Morris MJ, Stadler WM, et al. Trial design and objectives for castration-resistant prostate cancer: updated recommendations from the Prostate Cancer Clinical Trials Working Group 3. J Clin Oncol. 2016; 34:1402. [PubMed: 26903579]
24. Ravert HT, Holt DP, Chen Y, et al. An improved synthesis of the radiolabeled prostate-specific membrane antigen inhibitor, [$^{18}$F]DCFPyL. J Label Compd Radiopharm. 2016; 59:439.
25. Fendler WP, Calais J, Allen-Auerbach M, et al. $^{68}$Ga-PSMA-11 PET/CT interobserver agreement for prostate cancer assessments: an international multicenter prospective study. J Nucl Med. 2017; doi: 10.2967/jnumed.117.190827
26. Budäus L, Leyh-Bannurah S-R, Salomon G, et al. Initial experience of $^{68}$Ga-PSMA PET/CT imaging in high-risk prostate cancer patients prior to radical prostatectomy. Eur Urol. 2016; 69:393. [PubMed: 26116958]
27. Herlemann A, Wenter V, Kretschmer A, et al. $^{68}$Ga-PSMA positron emission tomography/computed tomography provides accurate staging of lymph node regions prior to lymph node dissection in patients with prostate cancer. Eur Urol. 2016; 70:553. [PubMed: 26810345]
28. Maurer T, Gschwend JE, Rauscher I, et al. Diagnostic efficacy of $^{68}$gallium-PSMA positron emission tomography compared to conventional imaging for lymph node staging of 130 consecutive patients with intermediate to high risk prostate cancer. J Urol. 2016; 195:1436. [PubMed: 26682756]
29. van Leeuwen PJ, Emmett L, Ho B, et al. Prospective evaluation of $^{68}$gallium-prostate-specific membrane antigen positron emission tomography/computed tomography for preoperative lymph node staging in prostate cancer. BJU Int. 2017; 119:209. [PubMed: 27207581]
30. Barinka C, Byun Y, Dusich CL, et al. Interactions between human glutamate carboxypeptidase II and urea-based inhibitors: structural characterization. J Med Chem. 2008; 51:7737. [PubMed: 19053759]

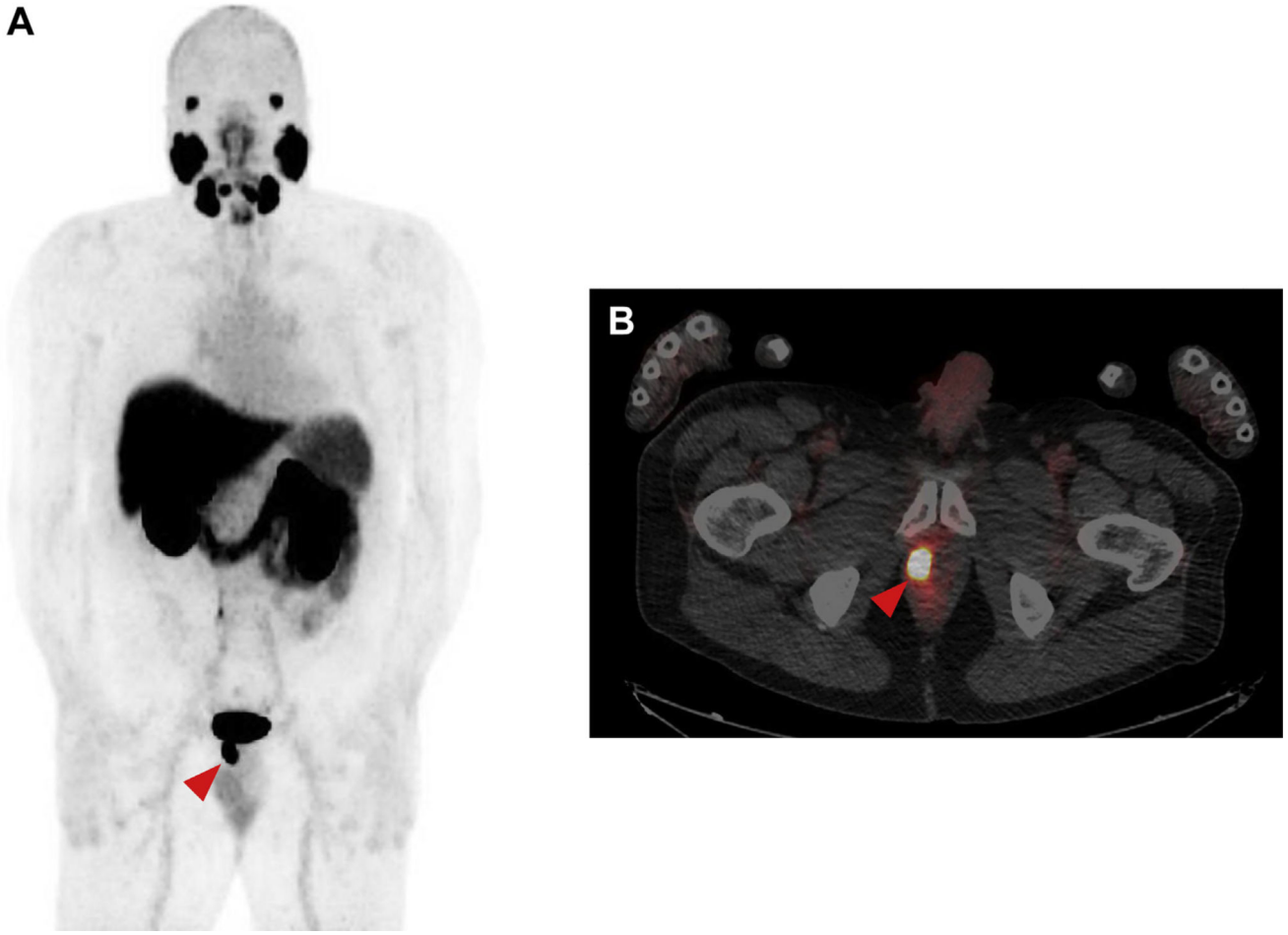


**Figure 1.**

Normal biodistribution of $^{18}$F-DCFPyL with additional focal uptake in prostate. Normal biodistribution of radiotracer includes uptake in lacrimal and salivary glands, oropharynx, kidneys, liver, proximal small bowel, spleen, ureters and bladder. Focal uptake in prostate (red arrows, $SUV_{max}$ = 26.7) is consistent with prostate cancer site. At radical prostatectomy Gleason 4 + 5 = 9 pT2 prostate cancer was found in right side of prostate. *A*, maximal intensity projection. *B*, axial fused PET/CT images.

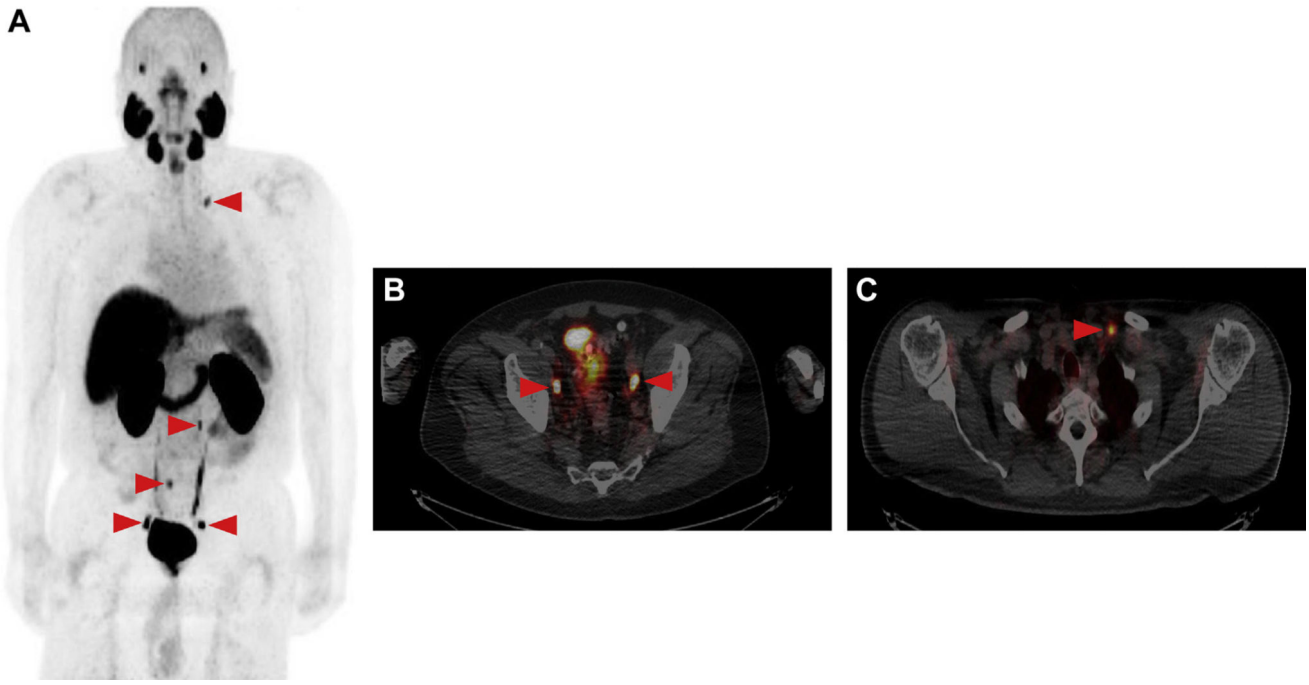


**Figure 2.**

Representative images of patient with suspected regional and distant lymph node metastases (N1 and M1a) detected on preoperative $^{18}$F-DCFPyL PET/CT. Note multiple sites of focal radiotracer uptake (red arrows, $SUV_{max}$ values greater than 3.5). At radical prostatectomy Bilateral pelvic lymph node metastases were found at radical prostatectomy. *A*, maximal intensity projection. *B* and *C*, axial fused PET/CT.

**Table 1**

Study cohort demographic and clinical characteristics, and surgical pathology data

| | | |
|---|---|---|
| No. pts | 25 | |
| Median age (range) | 61 | (49–75) |
| No. race (%): | | |
| White | 20 | (80) |
| Black | 2 | (8) |
| Other | 3 | (12) |
| Median preop ng/ml PSA (range) | 9.3 | (3.6–125.5) |
| No. biopsy Gleason score (%): | | |
| 3 + 4 = 7 | 1 | (4) |
| 3 + 5 = 8 | 3 | (12) |
| 4 + 4 = 8 | 8 | (32) |
| 4 + 5 = 9 | 12 | (48) |
| 5 + 4 = 9 | 1 | (4) |
| No. clinical T stage (%): | | |
| cT1c | 11 | (44) |
| cT2a | 7 | (28) |
| cT2b | 3 | (12) |
| cT2c | 4 | (16) |
| No. NCCN risk category (%): | | |
| High | 17 | (68) |
| Very high | 8 | (32) |
| No. dominant nodule Gleason score (%): | | |
| 4 + 3 = 7 | 5 | (20) |
| 4 + 4 = 8 | 2 | (8) |
| 4 + 5 = 9 | 17 | (68) |
| 5 + 4 = 9 | 1 | (4) |
| No. pathological T stage (%): | | |
| pT2 | 4 | (16) |
| pT2x | 1 | (4) |
| pT3a | 13 | (52) |
| pT3b | 7 | (28) |
| No. surgical margin status (%): | | |
| Neg | 17 | (68) |
| Pos | 8 | (32) |
| Median No. removed lymph nodes (range) | 13 | (5–45) |
| No. overall pathological N stage (%): | | |
| pN0 | 18 | (72) |
| pN1 | 7 | (28) |
| No. lt hemipelvis pathological N stage (%): | | |
| pN0 | 21 | (84) |

| | | |
|---|---|---|
| pN1 | 4 | (16) |
| No. rt hemipelvis pathological N stage (%): | | |
| pN0 | 20 | (80) |
| pN1 | 5 | (20) |

**Table 2**

Diagnostic performance of $^{18}$F-DCFPyL PET/CT for detecting pelvic lymph node metastases

| Analysis Level | % (95% CI) |
|---|---|
| Pt: | |
| Sensitivity | 71.4 (29.0–96.3) |
| Specificity | 88.9 (65.3–98.6) |
| Pos predictive value | 71.4 (38.4–90.9) |
| Neg predictive value | 88.9 (71.0–96.3) |
| Packet: | |
| Sensitivity | 66.7 (29.9–92.5) |
| Specificity | 92.7 (80.1–98.5) |
| Pos predictive value | 66.7 (38.0–86.7) |
| Neg predictive value | 92.7 (83.4–97.0) |